Published in final edited form as:
Cell. 2011 April 15; 145(2): 312–321. doi:10.1016/j.cell.2011.03.013.

Thermal robustness of signaling in bacterial chemotaxis

Olga Oleksiuk[1,†], **Vladimir Jakovljevic**[1,†], **Nikita Vladimirov**[1], **Ricardo Carvalho**[1], **Eli Paster**[2], **William S. Ryu**[2,‡], **Yigal Meir**[3], **Ned S. Wingreen**[2,4], **Markus Kollmann**[5], and **Victor Sourjik**[1,*]

[1] Zentrum für Molekulare Biologie der Universität Heidelberg, DKFZ-ZMBH Alliance, Im Neuenheimer Feld 282, D-69120 Heidelberg, Germany

[2] Lewis-Sigler Institute for Integrative Genomics, Princeton University, Princeton, New Jersey 08544, USA

[3] Department of Physics, Ben Gurion University, Beer Sheva 84105, Israel

[4] Department of Molecular Biology, Princeton University, Princeton, New Jersey 08544-1014, USA

[5] Heinrich-Heine-Universität Düsseldorf, Department of Biology, Universitätsstr. 1, D-40225 Düsseldorf, Germany

Summary

Temperature is a global factor that affects the performance of all intracellular networks. Robustness against temperature variations is thus expected to be an essential network property, particularly in organisms without inherent temperature control. Here we combine experimental analyses with computer modeling to investigate thermal robustness of signaling in chemotaxis of *Escherichia coli*, a relatively simple and well-established model for systems biology. We show that steady-state and kinetic pathway parameters that are essential for chemotactic performance are indeed temperature-compensated in the entire physiological range. Thermal robustness of steady-state pathway output is ensured at several levels by mutual compensation of temperature effects on activities of individual pathway components. Moreover, the effect of temperature on adaptation kinetics is counterbalanced by pre-programmed temperature dependence of enzyme synthesis and stability to achieve nearly optimal performance at the growth temperature. Similar compensatory mechanisms are expected to ensure thermal robustness in other systems.

INTRODUCTION

Escherichia coli chemotaxis is one of the most thoroughly studied biological processes. *E. coli* performs chemotaxis by making short-term temporal comparisons of chemoeffector concentration (Berg and Brown, 1972; Berg and Purcell, 1977; Macnab and Koshland, 1972). When adapted in the absence of a gradient, swimming bacterial cells constantly alternate nearly straight runs with brief tumbles during which direction changes, thus

*Contact: v.sourjik@zmbh.uni-heidelberg.de.
†These authors equally contributed to this work
‡Present address: Department of Physics, Banting and Best Department of Medical Research, University of Toronto, Toronto M5S 1A7, Ontario, Canada

exploring their environment via an effective random walk. In *E. coli*, running and tumbling correspond to counterclockwise (CCW) and clockwise (CW) directions of flagellar motor rotation, respectively. In the presence of a chemoattractant gradient, changes in swimming direction are suppressed in cells swimming up the gradient by virtue of cells constantly comparing their current conditions with the level of stimulation several seconds ago.

The signal transduction pathway that mediates these temporal comparisons is well understood on the molecular level (Figure 1), recently reviewed in (Sourjik and Armitage, 2010). Chemoeffector stimuli are detected by sensory complexes, which consist of transmembrane receptors, a histidine kinase CheA and a scaffold protein CheW, and form supramolecular clusters at the cell poles and along the cell body. Receptors of different ligand specificities and in different modification states are mixed in these complexes and allosterically interact to amplify and integrate chemotactic stimuli at the level of CheA activity (Ames et al., 2002; Li and Weis, 2000; Sourjik and Berg, 2004). The signal is transduced to the flagellar motors through the phosphorylation of a small response-regulator protein CheY, which in its phosphorylated form, CheY-P, binds to the motors and induces a switch to the clockwise (CW) direction of rotation, leading to a tumble and reorientation. Methylation of receptors on four specific glutamate (E) residues by the methyltransferase CheR, and their demethylation by the methylesterase CheB, slowly offset the effect of ambient stimulation on receptor activity and restores the adapted level of CheY-P. The slow kinetics of receptor methylation provides the short-term memory for temporal concentration comparisons (Vladimirov and Sourjik, 2009).

Signal processing by the receptor-kinase complexes can be described in terms of the allosteric two-state model, where the kinase activity of a complex is proportional to the equilibrium probability of the active state, P_{on} (Keymer et al., 2006; Mello and Tu, 2005). At a defined temperature, an increased level of receptor methylation, or a similarly neutralizing replacement of glutamate residues with glutamine (Q), results in a gradual increase in receptor activity, whereby P_{on} is close to unity for fully modified receptors and close to zero for fully unmodified receptors (Endres et al., 2008; Morton-Firth et al., 1999). Ligand binding decreases P_{on} in a concentration-dependent manner (Keymer et al., 2006; Mello and Tu, 2005; see also Eqs. [1–4] in Supplemental Experimental Procedures – Modeling), with $P_{on} \approx 0$ at saturating stimulation even for high levels of receptor modification. The ligand concentration required for a half-maximal response to step-changes in attractant concentrations, EC_{50}, increases monotonically with receptor modification (Endres et al., 2008; Li and Weis, 2000; Sourjik and Berg, 2002b), meaning that higher-modified receptors are more active and less sensitive to ligands. An average modification level of mixed wild-type complexes in the absence of ligand is around one group per receptor (Endres et al., 2008) corresponding to an intermediate level of the receptor-kinase complex activity ($P_{on} \sim 0.3$), which apparently ensures that receptor-kinase complexes are in the highly sensitive regime with $P_{on} \leq 0.5$ (Keymer et al., 2006). Given that CheR preferentially methylates inactive receptors and CheB preferentially demethylates active receptors, the adaptation kinetics of this system can be described as $dm/dt = \gamma_R[1 - P_{on}(t)] - \gamma_B P_{on}(t)$, where m is the mean methylation level per receptor dimer, and γ_R and γ_B are the maximal methylation and demethylation rates, respectively (Barkai and Leibler, 1997; Meir et al., 2010). The resulting adaptation maintains a steady state of activity that is nearly invariant over several orders of magnitude of attractant concentration (Alon et al., 1999; Barkai and Leibler, 1997; Neumann et al., 2010).

The corresponding level of the steady-state output signal, CheY-P, is one of the two parameters most crucial for optimal chemotactic behavior. CheY-P has to be maintained in the narrow operating range of the flagellar motor (Cluzel et al., 2000) to maximize motor response to small changes in pathway activity, and even a minor deviation from this optimal

level of CheY-P can lead to a substantial decrease in the efficiency of chemotaxis (Løvdok et al., 2009; Vladimirov et al., 2008). The other crucial parameter is adaptation kinetics, which sets the time scale of temporal comparisons made by cells swimming in gradients. It was shown that optimal chemotaxis in a given gradient requires a well-defined adaptation time, which depends on the swimming velocity and rotational diffusion of bacteria (Andrews et al., 2006; Berg and Purcell, 1977; Vladimirov et al., 2008).

Because of its relative simplicity, clearly defined performance objectives and abundance of quantitative information, *E. coli* chemotaxis has been extensively used as a model for theoretical and experimental analyses of general properties of cellular systems. Several studies suggested that chemotaxis operates close to a theoretical limit of sensitivity (Berg and Purcell, 1977; Bialek and Setayeshgar, 2005; Endres et al., 2008), making it one of the best-studied examples of evolutionary optimization. Another much analyzed property of the chemotaxis pathway is its robustness against such perturbations as variations in ambient stimulation and protein levels (Alon et al., 1999; Barkai and Leibler, 1997; Kollmann et al., 2005; Løvdok et al., 2009). Robustness is believed to be one of the most universal evolutionarily selected properties of cellular networks, and the underlying mechanisms of robustness show analogy to universal engineering concepts (Kitano, 2007; Stelling et al., 2004), but few examples of detailed robustness analyses exist.

The goal of this study was to investigate robustness of the *E. coli* chemotaxis pathway against variations in ambient temperature, one of the most common natural perturbation factors. Although thermal robustness is expected to be a common property of cellular networks, the only cellular systems analyzed so far in this context are circadian clocks (Virshup and Forger, 2009), and no systematic analysis of temperature effects on any signaling network is yet available. *E. coli* is a normal constituent of human microflora but is also found in soil and water, and is therefore expected to perform chemotaxis over a wide temperature range, making the chemotaxis pathway a well-suited model to understand the general mechanisms underlying thermal robustness of signaling.

The analysis of thermal robustness of *E. coli* chemotaxis is particularly interesting because temperature is also a known stimulus for the chemotaxis pathway (Maeda et al., 1976). A temperature increase elicits a transient attractant-like response (i.e., decrease in the kinase activity) below 37°C and a repellent-like response (i.e., increase in the kinase activity) above this temperature (Paster and Ryu, 2008). This sign inversion of the thermotactic response enables cells to accumulate at a preferred temperature, 37°C. Chemotactic and thermotactic responses are both mediated by chemoreceptors and adaptation to chemoattractant stimuli that increases receptor methylation can invert the sign of the thermotactic response even below 37°C (Mizuno and Imae, 1984; Nara et al., 1996; Paster and Ryu, 2008; Salman and Libchaber, 2007). Importantly, highly sensitive thermotaxis and temperature- compensated chemotaxis do not have to be mutually exclusive. The pathway response to temperature is only transient (Maeda et al., 1976; Paster and Ryu, 2008), and bacteria may therefore perform thermotaxis by responding to small rapid changes in temperature experienced during cell movement in a thermal gradient and yet be able to compensate the effects of slowly varying temperature on chemotaxis.

Here we showed that although ambient temperature indeed affects all individual steps in chemotactic signaling, both key pathway parameters – the steady-state output and adaptation kinetics – are temperature-compensated. The observed mechanisms of temperature compensation include (1) opposing temperature effects on the activity of individual receptors in mixed complexes and on sequential steps in signal transduction, (2) similar temperature dependences of opposing enzymatic reactions, and (3) counterbalancing of the effect of temperature on reaction rates via preprogrammed temperature dependence of

enzyme levels to achieve nearly optimal performance at the growth temperature. Similar mechanisms of thermal compensation and optimal adjustment of performance to the ambient temperature are expected to be common to many cellular networks.

RESULTS

Thermal Effects on Receptor Activity and Methylation

To determine the effects of temperature on activity and EC_{50} of the receptor-kinase complexes, we utilized an *in-vivo* CheY phosphorylation assay based on fluorescence resonance energy transfer (FRET) between fusions of CheY and CheZ to yellow and cyan fluorescent proteins, CheY-YFP and CheZ-CFP (Figure S1A–C) (Sourjik and Berg, 2002b, 2004; Sourjik et al., 2007). The *FRET* value measured in this assay – a fractional reduction in CFP fluorescence due to energy transfer to YFP in the complex formed between phosphorylated CheY-YFP and CheZ-CFP – is proportional to the relative intracellular amount of this complex, $[Y_PZ]/[Z]_T$, where $[Z]_T$ is the total intracellular concentration of CheZ-CFP. Since the steady-state value of $[Y_PZ]$ is itself determined by the balance of the phosphorylation and dephosphorylation reactions (Figure S1B), the value of FRET can be expressed in terms of reaction rates and protein concentrations in the chemotaxis pathway as $FRET = E_{FRET}k_A[A^C]P_{on}/k_Z[Z]_T$, where k_A and k_Z are the rate constants of CheA autophosphorylation and CheY-P dephosphorylation when complexed with CheZ, respectively, $[A^C]$ is the concentration of receptor-cluster-associated CheA, P_{on} is the equilibrium probability that the receptor-kinase complexes are in their active state, and E_{FRET} is the maximal FRET efficiency achieved when $[Y_PZ] = [Z]_T$ (see Supplemental Experimental Procedures for details of calculations). When the values of E_{FRET}, k_A, k_Z, $[A^C]$, and $[Z]_T$ are fixed, *FRET* provides a direct readout of the steady-state activity of the receptor- kinase complexes (P_{on}). *FRET* also reflects the steady-state level of free CheY-P, $[Y_P]$, in the cell, since $[Y_PZ] = k_{on}[Y_P][Z]/(k_{off}+ k_Z)$, where [Z] is the concentration of free CheZ, and k_{on} and k_{off} are the association and dissociation rates of the CheY-P•CheZ complex (Figure S1B).

We first used the FRET assay to analyze the effects of temperature on both major *E. coli* chemoreceptors, those for aspartate (Tar) and serine (Tsr). Receptors in defined modification states (carrying zero to four glutamines, which are functionally similar to methylated glutamates) were individually expressed from salicylate-inducible plasmid vectors in an otherwise receptor-less and modification-enzyme-deficient background. Since receptor properties are known to change monotonically with the number of modified residues (Endres et al., 2008), only properties of several representative states that span the whole range of modifications (EEEE, QEEE, QEQE, and QQQQ for Tar; EEEE, QEEE, and QQQQ for Tsr) rather than of all possible 16 permutations were investigated. To determine the basal level of FRET and the dose responses to attractant, cells were equilibrated in the buffer at a given temperature and subsequently stimulated with increasing steps of attractant, α-methyl-DL-aspartate (MeAsp) for Tar and L-serine for Tsr, returning to buffer before each subsequent attractant stimulation (Figure S1C). We observed that the level of FRET in the absence of stimulation decreased with increasing temperature in cells expressing Tar^{QEEE} but increased in cells expressing Tar^{QEQE} or Tar^{QQQQ} (Figure 2A). A similar inversion of the temperature effect was observed for Tsr, although it occurred instead between zero- and one-modified receptors (Figure S1D). Consistently, the values of EC_{50} – concentration of chemoattractant that elicited a half-maximal response –showed opposing dependence on temperature for low- and high-modified receptors (Figure 2B and Figure S1E). Altogether, these data demonstrate that Tar^{QEEE} and Tsr^{EEEE} are temperature inactivated, whereas Tar^{QQQQ} and Tsr^{QQQQ} are activated, confirming that the thermal effect on receptor activity depends on the state of receptor modification (Mizuno and Imae, 1984; Nara et al., 1996; Nishiyama et al., 1997; Salman and Libchaber, 2007). A detailed analysis of our data using

the allosteric model of receptor clusters is presented in Supplemental Experimental Procedures – Modeling and in Figure S1F, G.

In principle, because sensory complexes in adapted $CheR^{+}CheB^{+}$ cells contain a mixture of different receptor modification states, the opposing temperature effects on the individual modification states can largely compensate each other to maintain temperature-independent output. To explore whether this strategy is likely to be used, we analyzed the extent of Tar methylation in $CheR^{+}CheB^{+}$ cells adapted to different temperatures in the absence of ligand (Figure 2C). The average level of receptor modification in adapted cells was indeed around one group at all temperatures, close to the point where the sign of the temperature response inverts. This means that a change in temperature should only elicit a weak activity response and consequently requires little adaptive methylation.

To directly demonstrate such compensation, we co-expressed Tar^{QEEE} from a plasmid together with chromosomally-encoded Tar^{QEQQ} (Figure 2D). Consistent with the expected activating effect on high-modified receptors, FRET increased with temperature in Δ*tsr* cells expressing only chromosomally-encoded Tar^{QEQQ} (note that the genetic background and Tar expression level in these cells slightly differ from those shown in Figure 2A). In contrast to this temperature activation, and also in contrast to the even more pronounced temperature inactivation of Tar^{QEEE} (Figure 2A), no significant change in FRET with temperature was observed for cells expressing a mixture of these two receptors, confirming mutual compensation of the temperature effects on individual receptors in mixed receptor complexes. Note that the near perfect compensation in this experiment required lower expression of Tar^{QEEE} compared to Tar^{QEQQ} (≈0.4:1), consistent with the stronger temperature effect on Tar^{QEEE}.

Direct Thermal Effects on Phosphatase and Kinase Activity

Unlike ligand stimulation that only affects specific receptor activity, temperature may also influence other parameters that contribute to overall pathway activity and to the FRET signal. There was no discernible direct effect of temperature on the efficiency of FRET, as determined by measuring FRET for a stable CheZ-YFP/CheZ-CFP dimer using acceptor photobleaching (Kentner and Sourjik, 2009; data not shown), which is consistent with the little change expected in the physical and chemical parameters within the explored temperature range. However, temperature dependence was found for both k_A and k_Z. To characterize the temperature dependence of k_Z, we measured kinetics of $[Y_PZ]$ decay by FRET upon fast, saturating stimulation with 1 mM L- aspartate (Figure S2A). While the observed decay rate at room temperature was consistent with previous estimates of *in-vivo* CheY-P dephosphorylation kinetics (Kentner and Sourjik, 2009; Sourjik and Berg, 2002a), the dephosphorylation rate increased significantly with higher temperature (Figure 3A and Figure S2A). This increase could be fit to an Arrhenius form $Ae^{\Delta E/kT}$, where A is a constant, ΔE is an activation energy of the dephosphorylation reaction, T is temperature in Kelvin, and k is the Boltzmann constant (Figure 3A *Inset*), yielding an estimated value of ΔE of ≈20 kJ mol^{-1}. Since the steady-state FRET amplitude is determined by the ratio $k_A P_{on}/k_Z$, the dependence of k_A on temperature can be estimated as the product of k_Z and *FRET* for the strain that expresses receptor in a high-modification state (Figure 2A and Figure S1C) and is therefore expected to have $P_{on} \approx 1$ at all temperatures. The resulting estimated increase of k_A with temperature was steeper than that of k_Z, corresponding to an activation energy of ≈40 kJ mol^{-1} (Figure S2B). This is similar to the average temperature dependence of most enzymatic reactions, which approximately double their rate every 10°C.

Due to the differences in their activation energies, the increases in the rates of phosphorylation and dephosphorylation of CheY with temperature are only partly compensatory; the compensation of temperature effects by mixed receptor complexes is

apparently also imperfect. As a result, wild-type cells still show a significant increase in the steady-state level of FRET in the temperature range between 10 to 30°C (Figure 3B). Such imprecise temperature compensation may be required for effective thermotaxis towards a preferred temperature (Jiang et al., 2009), but this imprecision appears to present a problem for the robustness of chemotaxis. Because of the extreme steepness of the flagellar motor response, which has a Hill coefficient of ≈10 (Cluzel et al., 2000) even a minor variation in the steady-state level of CheY-P with temperature is expected to produce a large deviation from the optimal steady- state motor CW bias. Nevertheless, the observed change in the adapted motor bias with temperature (Paster and Ryu, 2008) is modest, comparable to the relative change in FRET (Figure 3B). This indicates temperature compensation at the level of the motor response, which is in accord with the previously observed decrease of motor sensitivity to active CheY with increasing temperature (Turner et al., 1999) (Figure 3B *Inset*).

Temperature Dependence of Adaptation Rate

Another central pathway parameter, adaptation time to a given attractant stimulus, showed a steep exponential decrease with temperature (Figure 4A). Although adaptation time to stronger stimuli was longer as expected, the effect of temperature was independent of the stimulation strength, yielding an apparent activation energy for the net rate of receptor methylation of ≈80 kJ mol^{-1} (Figure 4B). Because for the saturating attractant stimuli used here (which yield $P_{on} \approx 0$ for a large part of the time course of adaptation) the adaptation kinetics is dominated by the maximal activity of CheR (γ_R, see Introduction), our results suggest that γ_R increases by approximately threefold for each 10°C. The kinetics of adaptation to the removal of the corresponding saturating amounts of attractant, which reflects the net rate of receptor demethylation and is dominated by the activity of CheB, showed a similarly steep temperature dependence with the estimated average value of ΔE being ≈64 kJ mol^{-1} (Figure 4B). Given the general form of adaptation kinetics in chemotaxis (see Introduction), the observed temperature dependence of adaptation kinetics to strong stimuli should similarly apply to weak stimuli experienced by cells swimming in a gradient. Indeed, this temperature dependence can explain why weak time-varying attractant stimuli are sensed by the chemotaxis system with a threefold higher threshold frequency at 32°C compared to 22°C (Shimizu et al., 2010). Slight differences in the temperature dependences of γ_R and γ_B could explain the gradual shift in the adapted level of receptor methylation with temperature (Figure 2C). Nevertheless, the similarity of the activation energies and their values well above those of typical enzymatic reactions suggest that the temperature dependences of the methylation and demethylation reactions have co-evolved to provide yet another level of mutual compensation.

Temperature Dependence of Swimming Velocity

As mentioned above, there is a defined optimal adaptation rate for chemotaxis in a particular gradient, which is primarily determined by the swimming velocity of bacteria so that faster swimming requires a higher adaptation rate (see Supplemental Experimental Procedures – Modeling for details). We therefore determined the temperature dependence of the swimming velocity of *E. coli* by tracking adapted cells (Figure 5) and showed that the velocity moderately increases with temperature, consistent with previous measurements for *Streptococcus* (Lowe et al., 1987), and with the twofold decrease in the viscosity of water within this temperature range. As a result, the optimal adaptation rate is expected to increase only twofold for a temperature increase of 20°C, much less than the steep ninefold increase in the adaptation rate measured in this temperature range for a given population of bacteria.

Growth-Temperature Dependent Compensation of Adaptation Kinetics

What mechanisms could compensate for this mismatch? Since higher organisms, such as *C. elegans*, can modulate their behavior to match their feeding temperature (Hedgecock and Russell, 1975), we explored the possibility that the adaptation rate in bacterial chemotaxis might be similarly adjusted by growth temperature. Indeed, we observed that adaptation kinetics was slower for cultures grown at higher temperature (Figure 6A). As a result, the adaptation rate measured at the growth temperature of the respective culture was much less temperature sensitive than the adaptation rate of one culture grown at a fixed temperature of 37°C (Figure 6B). This suggests a compensatory mechanism whereby the increase in the rate of receptor methylation at high temperature is partly compensated by some property of cells grown at this temperature. Strikingly, the residual temperature dependence measured for the growth-temperature-compensated adaptation rate closely follows the theoretical optimum, which was either analytically calculated based on the temperature dependence of the swimming velocity (Figure 5) or simulated based on the swimming velocity and the steady-state bias (Figure 3B; see also Experimental Procedures and Supplemental Experimental Procedures – Modeling).

Regulation of Protein Levels by Growth Temperature

To investigate the origin of the growth-temperature-dependent compensation of the adaptation kinetics, we quantified relative intracellular levels of the adaptation enzymes CheR and CheB and of the receptors Tar and Tsr at different growth temperatures using quantitative immunoblotting. The levels of CheR and CheB were strongly affected by growth temperature, and to a similar extent, whereas the levels of receptors changed only little (Figure 7A and Figure S3A). This suggests that the dependence of the adaptation kinetics on the growth temperature could be explained by the change in the ratio of adaptation enzymes to their receptor substrates. We confirmed this by measuring the adaptation rate for a culture grown at a fixed temperature but with varying levels of CheR and CheB expression from a bicistronic plasmid construct that encodes both genes as one transcript and allows for their proportional induction. It is apparent that the dependence of the adaptation rate for this culture on the relative ratio of CheR to receptors closely matches the dependence observed in Figure 6A for the cultures grown at different temperatures (Figure 7B). Furthermore, no decrease in the adaptation rate with growth temperature was observed for cells with fixed levels of plasmid-expressed CheR and CheB (Figure S3B).

Since *cheR*, *cheB*, and *tar* are cotranscribed in *E. coli* as one polycistronic mRNA from the *meche* operon, the temperature-dependent regulation of the ratio between methylation enzymes and receptors is likely to occur at the posttranscriptional level. Focusing on CheR, we investigated this regulation in detail. Consistent with our expectations, there was no significant change in the level of *cheR* mRNA relative to that of *tar* or *tsr* upon an increase in growth temperature from 27°C to 37°C (Figure 7C). In contrast, we observed gene-specific temperature effects on synthesis of translational YFP reporter constructs. Whereas the synthesis of Tar-YFP under the native ribosome binding site (RBS) and of CheR-YFP under the core of its RBS (first 13 nucleotides upstream of the start codon) did not significantly change with temperature, the synthesis of CheR-YFP from a construct that included a large upstream fragment of the *meche* operon encoding the preceding *tap* gene showed a clear increase at lower temperature (Figure 7D). Since the levels of mRNA for these constructs were similar at 27°C and 37°C (measured using real-time PCR, data not shown), this differential regulation of protein levels with temperature must arise from translational control of *cheR*, whereby the upstream fragment preferentially upregulates the level of CheR translation at 27°C. To ensure that this regulation does not happen on the posttranslational level, we confirmed that the extent of degradation of YFP in all samples in a generation time (60 min at 37°C and 96 min at 27°C) was approximately the same at both

temperatures (≈20%; data not shown). We further mapped the region responsible for the observed translational regulation to approximately 100 nucleotides upstream of the *cheR* start codon. Although the details remain to be understood, the regulation might be related to the secondary mRNA structure predicted in this region (Figure S3C). This structure exposes the Shine- Dalgarno (SD) sequence of *cheR* and may therefore have a positive effect on the binding of ribosomes and on translation initiation, particularly at lower temperature when the mRNA structure is more stable. It has to be noted that the endogenous SD sequence of *cheR* is apparently very poor, whereby a single spontaneous nucleotide deletion in the SD region was observed to increase CheR translation by nearly 30 fold at 34°C (V.S., unpublished). Efficiency and selectivity of the upregulation of *cheR* synthesis by the upstream region appears to further require translation of *tap*, as elimination of the start codon of *tap* by site-directed mutagenesis largely decreased the expression level of CheR-YFP fusion, although higher relative translation at 37°C was retained in this construct. Such positive effect of translation might stem from the resolution of alternative secondary structure(s) further upstream of *cheR*, allowing a more efficient formation of the proposed regulatory structure immediately 5′ of the start codon. As yet another indication of the mRNA structure involvement, point mutations that destabilized predicted secondary structure upstream of *cheR* (Figure S3C) eliminated the selective upregulation of CheR-YFP translation at low temperature (Figure 7D).

As an additional level of regulation, the levels of endogenous receptors and CheR are differentially affected by temperature-dependent proteolysis (Figure 7E and Figure S3D). Although the extent of proteolysis was minor at 27°C, <10% for CheR and <20% for receptors in one hour, the proteolysis rate increased significantly at 37°C, up to 50% in one hour for both proteins. Thus, even considering the difference in the generation time (see above), degradation will have a larger impact on the steady-state levels of proteins at 37°C. More importantly, this increase in proteolysis was more pronounced for CheR, meaning that degradation specifically reduces the ratio of CheR to receptors at higher temperatures. This differential temperature dependence of proteolysis might be partly explained by differences in protease systems that degrade receptors and CheR, whereby only receptors are specifically degraded by Lon protease (Figure 7F). In addition, it is possible that thermolability of the CheR structure is generally higher. Combined, the observed differential regulation of translation and proteolysis of *cheR* and receptors can fully account for the specific decrease in the ratio of CheR to receptor levels at higher growth temperature.

DISCUSSION

The universal need to compensate the output function against temperature variation is expected to have shaped the evolution of most cellular networks. However, the only examples of thermal robustness that have been analyzed so far are circadian clocks (Virshup and Forger, 2009), and the mechanisms that ensure temperature compensation in other networks remain unknown. In this study, we investigated the effects of temperature and mechanisms of temperature compensation in the signaling network of *E. coli* chemotaxis, one of the most studied models for analyses of robustness and evolutionary optimization. We showed that although temperature affects multiple aspects of signal processing in chemotaxis, including all kinetic rates and the activity states of chemoreceptors and of the flagellar motor (Figure 1), the key steady-state and kinetic pathway parameters are kept within the narrow ranges optimal for chemotaxis in the domain of physiological temperatures, thus making the system as a whole robust to variations in ambient temperature.

Thermal Robustness of the Steady-state Output

The *E. coli* chemoreceptors adaptively respond to changes in temperature (Maeda et al., 1976; Paster and Ryu, 2008), which allows cells to perform thermotaxis in temperature gradients. However, in contrast to chemical stimulation, perturbations caused by temperature are not restricted to receptor activity and therefore cannot be fully compensated by changes in receptor methylation. In this study, we demonstrate that temperature compensation of the steady-state level of CheY-P takes place at multiple levels. At the sensory complexes, compensation primarily occurs through the opposing temperature dependences of individual modification states of receptors. Since sensory complexes in adaptive cells contain a mixture of modification states, the sign and magnitude of the temperature response can in principle be tuned by varying the fractions of individual modification states in the complex to produce a temperature-invariant output. Consistent with that, the average modification level of receptors in cells adapted in the absence of chemoattractant is just below the level where the sign of the temperature response inverts, which apparently ensures that cells respond to temperature changes only weakly and do not need large changes in receptor methylation for adaptation. Maintaining a high steady-state number of free methylation sites independent of ambient temperature might be evolutionarily beneficial to ensure that the chemotaxis system retains its ability to adapt to high concentrations of attractants at all temperatures.

Temperature further directly affects the rates of both pairs of opposing reactions that determine the adapted level of CheY-P – phosphorylation/dephosphorylation of CheY and methylation/demethylation of receptors. Whereas the former rates increase by less than twofold over 10°C, within the range of temperature dependence observed for typical enzymatic reactions, the increase for the latter rates is substantially steeper. Although an unbalanced increase in any of these rates would strongly affect the steady-state level of CheY-P (Kollmann et al., 2005; Løvdok et al., 2009), similar temperature dependences of opposing reactions within each pair largely balance each other over the entire temperature range. These similarities within each pair indicate that the activation energies of reactions may well have co-evolved under selection for thermal robustness. Nevertheless, this compensation appears to be imperfect in the chemotaxis network and differences in the temperature dependences within each reaction pair favor a moderate increase in the level of CheY-P at higher temperature. Such residual increase of the pathway activity with temperature may be an evolutionarily selected property that is required for thermotaxis (Jiang et al., 2009). However, because even a modest increase in the steady-state CheY-P level could produce a dramatic change in the motor bias, it must be compensated at the level of motor control, which indeed occurs via reduction of the motor sensitivity towards CheY-P at high temperatures.

Growth-dependent Adjustment of the Adaptation Rate

The most interesting compensatory mechanism was observed for the central kinetic parameter of the pathway, the rate of adaptation. In contrast to the steady-state pathway output, temperature compensation of the adaptation kinetics is not an inherent property of the pathway structure. Because the optimal time scale of temporal comparisons in chemotaxis is defined by the ratio of the kinetics of receptor methylation to the swimming velocity of bacteria, the steep increase in the catalytic rate of CheR with temperature – much faster then the corresponding increase in the swimming velocity – makes it impossible for the same cells to efficiently follow chemical gradients of similar steepness at all temperatures. In simple terms, this problem arises because cells at high temperature reset their memory faster than they are able to move far enough along the gradient to experience a measurable change in ligand concentration.

To resolve this problem, cells apparently evolved a compensatory mechanism on a different level, by selectively regulating synthesis and stability of CheR relative to receptors in a growth temperature dependent manner. We observed that translation of CheR specifically increases at lower temperature, apparently controlled by mRNA secondary structure upstream of the *cheR* coding region, which may expose an otherwise poor SD sequence. Additional tuning occurs via a substantially increased rate of CheR degradation at higher growth temperature. As a result, the adaptation rate of cells at their respective growth temperature, which is the product of the rate constant and the enzyme concentration per receptor, is nearly temperature compensated. Moreover, the residual temperature dependence of this compensated adaptation rate closely matches the predicted theoretical dependence of the optimal rate. We also observed a similar variation in the levels of CheB with temperature, consistent with the need to balance the respective effects of both enzymes on the steady-state output (Kollmann et al., 2005; Løvdok et al., 2009). These results suggest that the relative expression of adaptation enzymes and receptors is pre-programmed by evolution to depend on the growth temperature in a way that ensures optimal chemotaxis at that particular temperature.

Conclusions

Altogether, our analysis demonstrates how thermally robust signaling can be achieved despite strong temperature dependencies of individual reactions and extends the understanding of bacterial chemotaxis as an evolutionarily optimized and robust system (Alon et al., 1999; Barkai and Leibler, 1997; Berg and Purcell, 1977; Endres et al., 2008; Kollmann et al., 2005; Løvdok et al., 2009). Our results illustrate two principal types of network parameters that have to be temperature compensated in signaling systems: steady-state parameters, exemplified by the signaling output in chemotaxis, and kinetic parameters, exemplified by the adaptation rate. We show that thermal robustness of the steady-state output in chemotaxis is achieved in a relatively straightforward way, through (1) opposing temperature effects on individual components of receptor complexes and on sequential steps in the pathway, and (2) through similar temperature effects on the activities of counteracting enzymes, kinase and phosphatase and methyltransferase and methylesterase, respectively. We expect that analogous mechanisms may ensure temperature-invariant output of most cellular networks, and compensation mediated by identical temperature dependences of opposing enzymatic reactions has indeed been proposed to explain thermal robustness of circadian clocks (Hastings and Sweeney, 1957; Huang et al., 1995; Mehra et al., 2009; Virshup and Forger, 2009). Moreover, compensatory coupling of opposing enzymatic activities appears to represent an even more general mechanism of robustness, since such coupling also ensures robustness of chemotaxis against gene expression noise (Kollmann et al., 2005; Løvdok et al., 2009).

Achieving thermal robustness of kinetic parameters is generally more difficult, because they depend directly on temperature (Rajan and Abbott, 2007). In chemotaxis, this problem is solved by the pre-programmed adjustment of enzyme levels with growth temperature, which allows bacteria to compensate the direct temperature dependence of the rate constants and ensures that cells optimally perform chemotaxis at their growth temperature. This supports the recent finding that bacteria can exhibit anticipatory behaviors (Tagkopoulos et al., 2008) and is likely to represent a general mechanism that allows an optimal adjustment of network function to the ambient temperature.

EXPERIMENTAL PROCEDURES

Strains and Plasmids

Escherichia coli K-12 strains, plasmids and primers used in this study are described in Tables S1 and S2. All FRET experiments were performed in Δ[*cheY cheZ*] background strains (VS104 or, where specified, its derivatives) that express CheY-YFP and CheZ-CFP fusions and, where specified, receptors or CheR and CheB.

Growth Conditions

E. coli cells were grown at 275 rpm in a rotary shaker to mid- exponential phase ($OD_{600} \approx 0.48$) in tryptone broth (TB) medium supplemented with appropriate antibiotics and inducers as described in Supplemental Experimental Procedures.

FRET Experiments

Cell preparation and FRET measurements were performed as described previously (Neumann et al., 2010; Sourjik and Berg, 2002b; Sourjik et al., 2007). Cells were attached to a polylysine-coated coverslip and placed into a flow chamber, mounted on a custom-modified microscope. Temperature in the flow chamber was controlled by a water bath and monitored using a thermocouple. The chamber was maintained under a constant flow (0.5 ml/min) of tethering buffer by a syringe pump. The same flow was used to add and remove specified amounts of attractant in tethering buffer. Cells were adapted for at least 10 min to each ambient temperature prior to stimulation. Fluorescence of a field of 300–500 cells was continuously recorded in cyan and yellow channels using photon counters with 0.5 sec integration time. Faster flow (1 ml/min) and shorter integration time (0.03 sec) were used for measurements of response kinetics (Kentner and Sourjik, 2009). FRET was defined as a fractional change in CFP fluorescence due to energy transfer, and calculated from changes in the ratios of yellow and cyan fluorescence signals upon stimulation as described before (Sourjik et al., 2007). See Supplemental Experimental Procedures and Figure S1A–C for details of FRET measurements and calculation.

Quantification of Protein and mRNA Levels

The levels of receptor, CheR, and CheB and the extent of receptor methylation were determined using quantitative immunoblotting as described recently (Neumann et al., 2010). Relative expression of fluorescently tagged proteins was quantified using flow cytometry as described previously (Løvdok et al., 2009). Relative levels of mRNA were quantified using realtime PCR with primer pairs specific for the gene of interest (Table S2). For details, see Supplemental Experimental Procedures.

Cell Tracking Experiments

Cell tracking experiments were performed in a custom- made flow chamber mounted on a phase microscope equipped with a CMOS video camera (Basler A602f). Custom software written in LabVIEW (National Instruments) captured images of the swimming bacteria at 60 frames per second. The images were then analyzed off line using custom software written with MATLAB (Mathworks) to determine the swimming speed during run intervals. For details, see Supplemental Experimental Procedures.

Computer Simulations and Mathematical Modeling

Simulation of chemotactic efficiency in gradients and correction of the EC_{50} values in $CheR^{+}CheB^{+}$ strain (Figure 2B) for adaptation was performed using RapidCell simulator (Vladimirov et al., 2010; Vladimirov et al., 2008) as described in Supplemental

Experimental Procedures and with parameters given in Table S3. Details of mathematical analysis are described in Supplemental Experimental Procedures – Modeling.

Supplementary Material

Refer to Web version on PubMed Central for supplementary material.

Acknowledgments

We thank G. Schwarz und A. Müller for help with cloning, L. Turner for sharing data and R. Endres and M. Mayer for valuable discussions. This work was supported by grant GM082938 from the National Institutes of Health and in parts by grant SO 421/3-3 from the Deutsche Forschungsgemeinschaft and by the C.H.S.-Foundation.

References

Alon U, Surette MG, Barkai N, Leibler S. Robustness in bacterial chemotaxis. Nature. 1999; 397:168–171. [PubMed: 9923680]

Ames P, Studdert CA, Reiser RH, Parkinson JS. Collaborative signaling by mixed chemoreceptor teams in *Escherichia coli*. Proc Natl Acad Sci USA. 2002; 99:7060–7065. [PubMed: 11983857]

Andrews BW, Yi TM, Iglesias PA. Optimal noise filtering in the chemotactic response of *Escherichia coli*. PLoS Comput Biol. 2006; 2:e154. [PubMed: 17112312]

Barkai N, Leibler S. Robustness in simple biochemical networks. Nature. 1997; 387:913–917. [PubMed: 9202124]

Berg HC, Brown DA. Chemotaxis in *Escherichia coli* analysed by three-dimensional tracking. Nature. 1972; 239:500–504. [PubMed: 4563019]

Berg HC, Purcell EM. Physics of chemoreception. Biophys J. 1977; 20:193–219. [PubMed: 911982]

Bialek W, Setayeshgar S. Physical limits to biochemical signaling. Proc Natl Acad Sci USA. 2005; 102:10040–10045. [PubMed: 16006514]

Cluzel P, Surette M, Leibler S. An ultrasensitive bacterial motor revealed by monitoring signaling proteins in single cells. Science. 2000; 287:1652–1655. [PubMed: 10698740]

Endres RG, Oleksiuk O, Hansen CH, Meir Y, Sourjik V, Wingreen NS. Variable sizes of *Escherichia coli* chemoreceptor signaling teams. Mol Syst Biol. 2008; 4:211. [PubMed: 18682701]

Hastings JW, Sweeney BM. On the mechanism of temperature independence in a biological clock. Proc Natl Acad Sci USA. 1957; 43:804–811. [PubMed: 16590089]

Hedgecock EM, Russell RL. Normal and mutant thermotaxis in the nematode *Caenorhabditis elegans*. Proc Natl Acad Sci USA. 1975; 72:4061–4065. [PubMed: 1060088]

Huang ZJ, Curtin KD, Rosbash M. PER protein interactions and temperature compensation of a circadian clock in *Drosophila*. Science. 1995; 267:1169–1172. [PubMed: 7855598]

Jiang L, Ouyang Q, Tu Y. A mechanism for precision-sensing via a gradient-sensing pathway: a model of *Escherichia coli* thermotaxis. Biophys J. 2009; 97:74–82. [PubMed: 19580745]

Kentner D, Sourjik V. Dynamic map of protein interactions in the *Escherichia coli* chemotaxis pathway. Mol Syst Biol. 2009; 5:238. [PubMed: 19156130]

Keymer JE, Endres RG, Skoge M, Meir Y, Wingreen NS. Chemosensing in *Escherichia coli*: two regimes of two-state receptors. Proc Natl Acad Sci USA. 2006; 103:1786–1791. [PubMed: 16446460]

Kitano H. Towards a theory of biological robustness. Mol Syst Biol. 2007; 3:137. [PubMed: 17882156]

Kollmann M, Løvdok L, Bartholome K, Timmer J, Sourjik V. Design principles of a bacterial signalling network. Nature. 2005; 438:504–507. [PubMed: 16306993]

Li G, Weis RM. Covalent modification regulates ligand binding to receptor complexes in the chemosensory system of *Escherichia coli*. Cell. 2000; 100:357–365. [PubMed: 10676817]

Løvdok L, Bentele K, Vladimirov N, Muller A, Pop FS, Lebiedz D, Kollmann M, Sourjik V. Role of translational coupling in robustness of bacterial chemotaxis pathway. PLoS Biol. 2009; 7:e1000171. [PubMed: 19688030]

Lowe G, Meister M, Berg HC. Rapid rotation of flagellar bundles in swimming bacteria. Nature. 1987; 325:637–640.

Macnab RM, Koshland DEJ. The gradient-sensing mechanism in bacterial chemotaxis. Proc Natl Acad Sci USA. 1972; 69:2509–2512. [PubMed: 4560688]

Maeda K, Imae Y, Shioi JI, Oosawa F. Effect of temperature on motility and chemotaxis of *Escherichia coli*. J Bacteriol. 1976; 127:1039–1046. [PubMed: 783127]

Mehra A, Shi M, Baker CL, Colot HV, Loros JJ, Dunlap JC. A role for casein kinase 2 in the mechanism underlying circadian temperature compensation. Cell. 2009; 137:749–760. [PubMed: 19450520]

Meir Y, Jakovljevic V, Oleksiuk O, Sourjik V, Wingreen NS. Precision and kinetics of adaptation in bacterial chemotaxis. Biophys J. 2010; 99:2766–2774. [PubMed: 21044573]

Mello BA, Tu Y. An allosteric model for heterogeneous receptor complexes: understanding bacterial chemotaxis responses to multiple stimuli. Proc Natl Acad Sci USA. 2005; 102:17354–17359. [PubMed: 16293695]

Mizuno T, Imae Y. Conditional inversion of the thermoresponse in *Escherichia coli*. J Bacteriol. 1984; 159:360–367. [PubMed: 6376475]

Morton-Firth CJ, Shimizu TS, Bray D. A free-energy-based stochastic simulation of the Tar receptor complex. J Mol Biol. 1999; 286:1059–1074. [PubMed: 10047482]

Nara T, Kawagishi I, Nishiyama S, Homma M, Imae Y. Modulation of the thermosensing profile of the *Escherichia coli* aspartate receptor tar by covalent modification of its methyl-accepting sites. J Biol Chem. 1996; 271:17932–17936. [PubMed: 8663384]

Neumann S, Hansen CH, Wingreen NS, Sourjik V. Differences in signalling by directly and indirectly binding ligands in bacterial chemotaxis. EMBO J. 2010; 29:3484–3495. [PubMed: 20834231]

Nishiyama S, Nara T, Homma M, Imae Y, Kawagishi I. Thermosensing properties of mutant aspartate chemoreceptors with methyl-accepting sites replaced singly or multiply by alanine. J Bacteriol. 1997; 179:6573–6580. [PubMed: 9352902]

Paster E, Ryu WS. The thermal impulse response of *Escherichia coli*. Proc Natl Acad Sci USA. 2008; 105:5373–5377. [PubMed: 18385380]

Rajan K, Abbott LF. Temperature-compensated chemical reactions. Phys Rev E. 2007; 75:022902.

Salman H, Libchaber A. A concentration-dependent switch in the bacterial response to temperature. Nat Cell Biol. 2007; 9:1098–1100. [PubMed: 17694049]

Shimizu TS, Tu Y, Berg HC. A modular gradient-sensing network for chemotaxis in *Escherichia coli* revealed by responses to time-varying stimuli. Mol Syst Biol. 2010; 6:382. [PubMed: 20571531]

Sourjik V, Armitage JP. Spatial organization in bacterial chemotaxis. EMBO J. 2010; 29:2724–2733. [PubMed: 20717142]

Sourjik V, Berg HC. Binding of the *Escherichia coli* response regulator CheY to its target measured in vivo by fluorescence resonance energy transfer. Proc Natl Acad Sci USA. 2002a; 99:12669–12674. [PubMed: 12232047]

Sourjik V, Berg HC. Receptor sensitivity in bacterial chemotaxis. Proc Natl Acad Sci USA. 2002b; 99:123–127. [PubMed: 11742065]

Sourjik V, Berg HC. Functional interactions between receptors in bacterial chemotaxis. Nature. 2004; 428:437–441. [PubMed: 15042093]

Sourjik V, Vaknin A, Shimizu TS, Berg HC. In vivo measurement by FRET of pathway activity in bacterial chemotaxis. Methods Enzymol. 2007; 423:363–391.

Stelling J, Sauer U, Szallasi Z, Doyle FJ 3rd, Doyle J. Robustness of cellular functions. Cell. 2004; 118:675–685. [PubMed: 15369668]

Tagkopoulos I, Liu YC, Tavazoie S. Predictive behavior within microbial genetic networks. Science. 2008; 320:1313–1317. [PubMed: 18467556]

Turner L, Samuel AD, Stern AS, Berg HC. Temperature dependence of switching of the bacterial flagellar motor by the protein CheY(13DK106YW). Biophys J. 1999; 77:597–603. [PubMed: 10388784]

Virshup DM, Forger DB. Keeping the beat in the rising heat. Cell. 2009; 137:602–604. [PubMed: 19450508]

Vladimirov N, Lebiedz D, Sourjik V. Predicted auxiliary navigation mechanism of peritrichously flagellated chemotactic bacteria. PLoS Comput Biol. 2010; 6:e1000717. [PubMed: 20333235]

Vladimirov N, Løvdok L, Lebiedz D, Sourjik V. Dependence of bacterial chemotaxis on gradient shape and adaptation rate. PLoS Comput Biol. 2008; 4:e1000242. [PubMed: 19096502]

Vladimirov N, Sourjik V. Chemotaxis: how bacteria use memory. Biol Chem. 2009; 390:1097–1104. [PubMed: 19747082]

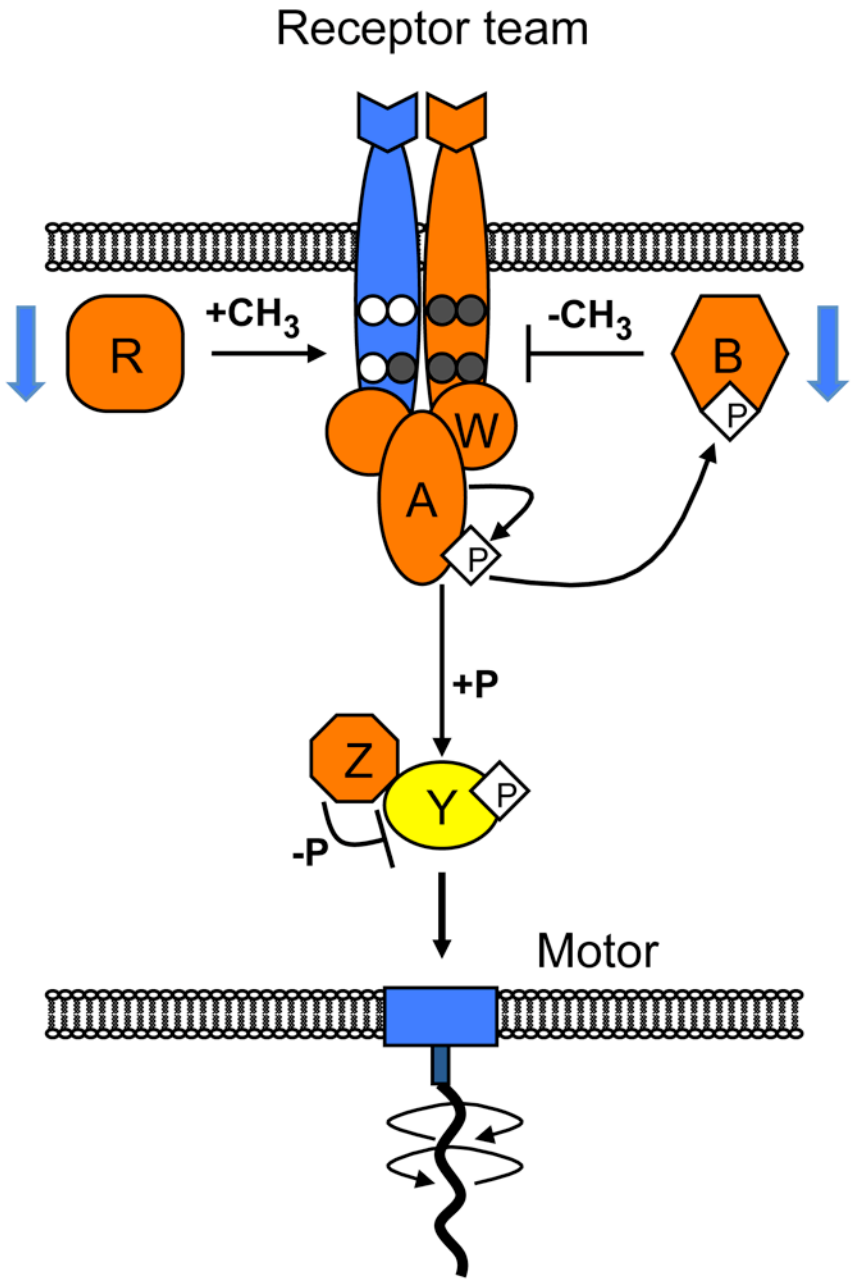

Figure 1. Signaling Pathway in *E. coli* Chemotaxis and Temperature Effects on Pathway Components

Sensory complexes consist of mixed teams of receptors (only one type of receptor is shown for simplicity) that jointly regulate the autophosphorylation activity of CheA with the help of an adaptor protein CheW. Receptors are methylated and demethylated/deamidated by the adaptation enzymes CheR and CheB, respectively, at four specific sites per receptor monomer (white circles, unmodified glutamates; dark grey circles, methylated glutamates or glutamines). The response regulator CheY is phosphorylated by CheA and dephosphorylated by CheZ. CheY-P binds to flagellar motors to induce a CW switch. Color code indicates temperature effects observed in this study: activation of proteins or protein complexes by increasing temperature is shown in orange and inactivation in blue. Together, CheA and

CheW are shown to be temperature-activated, because of the positive effect of temperature on kinase activity, although individual contributions of the two proteins were not characterized. An increase in the adapted level of CheY-P in wild-type cells is indicated in yellow. Blue arrows indicate the reduction in the expression levels of CheR and CheB with growth temperature.

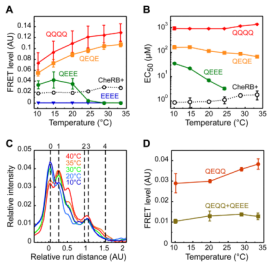

Figure 2. Temperature Effects on Chemoreceptor Activity and Methylation

(A, B) Temperature dependence of the pre-stimulus level of CheZ-CFP/CheY-YFP FRET **(A)** and of EC_{50} **(B)** for Tar expressed from a plasmid, as the sole receptor, either in $CheR^{+}CheB^{+}$ (VS181) or in *cheR cheB* (VH1) cells in one of the indicated modification states. Cells were pre-adapted to the test temperature in buffer and stimulated by step-like addition of varying amounts of MeAsp to determine dose responses. FRET was calculated from the changes in the YFP to CFP fluorescence ratio upon stimulation as illustrated in Figure S1C. The values of EC_{50} in $CheR^{+}CheB^{+}$ cells were corrected for partial adaptation during flow experiments. Note that EC_{50} for Tar^{EEEE} could not be determined. **(C)** Distribution of modification states of Tar expressed as the sole receptor in $CheR^{+}CheB^{+}$ (VS181 [pVS88/pVS123]) cells that were adapted to indicated temperatures in the buffer. Methylation was determined from the receptor mobility on an SDS-PAGE gel. Mobilities of Tar receptors with indicated number of glutamine substitutions (corresponding to EEEE, QEEE, QEQE, QEQQ, and QQQQ receptors) are shown by vertical dashed lines. Note that effects of modification on receptor mobility may depend on position of the modified residue, which presumably explains additional peaks observed between standards. The mobility of QEQE and QEQQ receptors is similar. The effect of modification on receptor mobility does not depend on the prior incubation temperature. All curves were normalized to their integral area. **(D)** Pre-stimulus FRET levels in VS150 cells expressing Tar^{QEQQ} from the native chromosomal location of the *tar* gene, or co-expressing it with Tar^{QEEE} encoded on a plasmid at a ratio Tar^{QEEE}:Tar^{QEQQ} of ≈0.4. Note that Tar^{QEQQ} cells still express low levels of minor receptors Trg and Aer, and also differ in the level of Tar expression from cells used in Figure 2A, which is likely to explain the differences in the FRET level and in the details of temperature dependence between the two experiments. Error bars here and throughout the paper (unless specified otherwise) indicate standard errors of multiple biological replicates. See Figure S1 and Experimental Procedures and Supplemental Experimental Procedures for details of experiments and analyses.

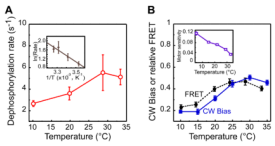

Figure 3. Temperature Effects on CheY Dephosphorylation Rate and on the Pathway Output

(A) Temperature dependence of CheY-P dephosphorylation rate. Dephosphorylation rate was determined by fitting kinetics of the FRET decay in VH1 [pVS123/pVS88] cells upon rapid stimulation with 1 mM asparate. *Inset* Arrhenius plot of the same data and the corresponding linear fit. **(B)** Adapted FRET level (black circles, scaled by 10^{-1} compared to units used in Figure 2) and CW motor bias (blue squares) taken from (Paster and Ryu, 2008) as functions of temperature for wild-type cells. *Inset* Temperature dependence of motor sensitivity, defined as the inverse of the concentration of a constitutively active mutant CheY** that produces a CW motor bias of 0.5, based on published data (Turner et al., 1999). Units of motor sensitivity are μM^{-1}. See also Figure S2.

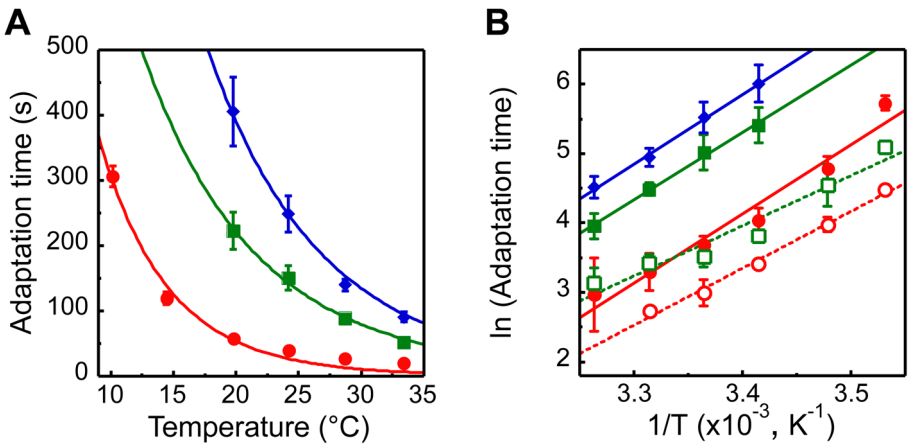

Figure 4. Adaptation Time as a Function of Temperature

(A) Adaptation time, defined as recovery time to half of the initial FRET level upon addition of 10 μM (red circles), 100 μM (green squares), or 300 μM (blue diamonds) of MeAsp, for cells grown at 34°C. Data are fitted using an Arrhenius form $Ae^{\Delta E/kT}$ (see text). **(B)** Arrhenius plot of the adaptation times in response to addition (closed symbols, replotted from A) and to subsequent removal (open symbols, same color code) of MeAsp after preceding adaptation. Data for removal of 300 μM MeAsp were not evaluated, because in most experiments adaptation to addition of this concentration was not followed until completion.

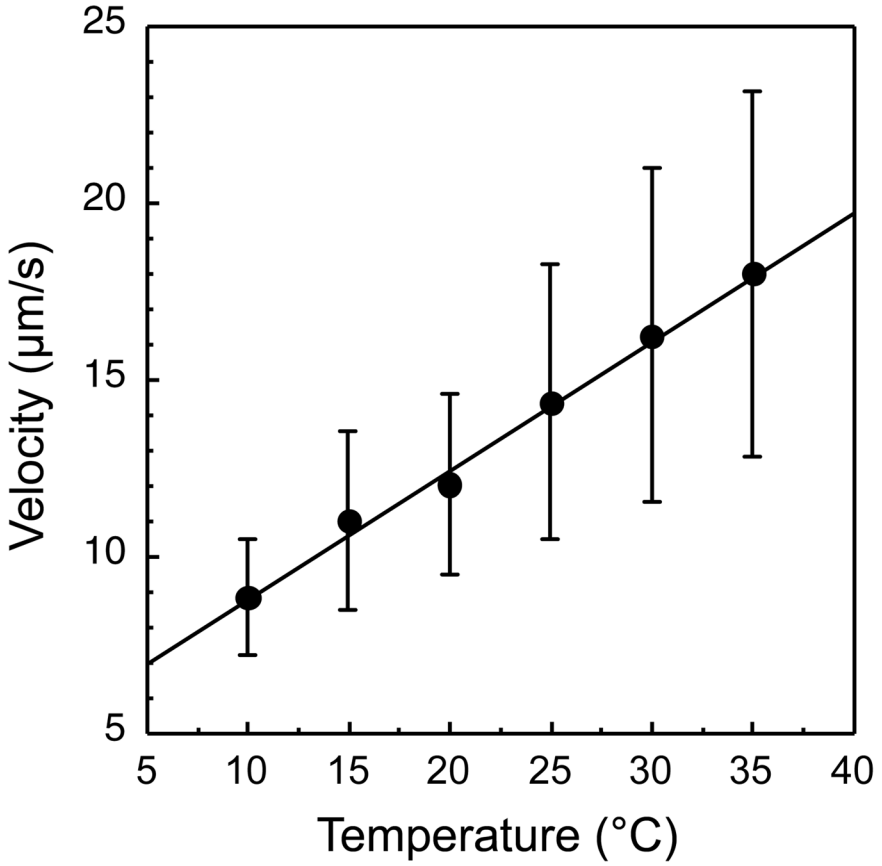

Figure 5. Swimming Velocity Dependence on Temperature

A dilute suspension of wild-type RP437 cells swimming near the coverslip surface was recorded at 60 fps using video phase microscopy. Swimming speed during runs was determined as described in Supplemental Experimental Procedures and averaged for each cell. Data from the population of 200–400 cells was then averaged for each temperature. Error bars indicate variation (standard deviation) among individual cells.

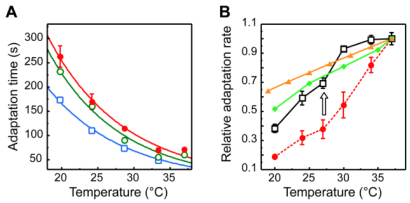

Figure 6. Growth Temperature Effects on Adaptation Kinetics

(A) Dependence of adaptation time (defined as in Figure 4) to 100 μM MeAsp on measurement temperature for cells grown at 37°C (red circles), 34°C (open green circles), and 30°C (open light blue squares). **(B)** Temperature dependence of the relative adaptation rate, defined as (adaptation time)$^{-1}$ for cells grown at 37°C (red circles) or at the respective measurement temperature (open black squares). As in all preceding figures, X axis indicates measurement temperature. Arrow indicates compensation of the adaptation rate by the growth temperature. Also shown is the optimal adaptation rate as a function of temperature, which was simulated (light green diamonds) or calculated (yellow triangles) as described in Supplemental Experimental Procedures. All values are normalized to the respective value at 37°C.

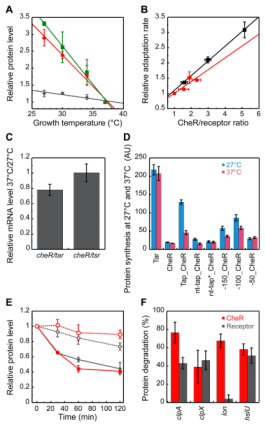

Figure 7. Growth Temperature Regulation of Protein Levels

(A) Dependence of relative levels of CheR (red circles), CheB (green squares), and receptors (grey diamonds) on the growth temperature. Protein levels were measured by quantitative immunoblotting as described in Supplemental Experimental Procedures. **(B)** Dependence of adaptation rate, determined for 100 μM MeAsp at 20°C as in Figure 6, on the relative CheR/receptor ratio. Wild-type cultures grown at 27, 30, 34 or 37°C are show with red circles; the values for 30 to 37°C were calculated from the data in Figure 6A. The 34°C culture with different levels of CheR and CheB induction (0.001%, 0.003% or 0.01% L-arabinose) from a bicistronic construct pV144 is shown with black squares. All values in (A, B) are normalized to the respective values for the 37°C culture. **(C)** Ratio of endogenous mRNA levels of indicated genes in cultures of wild-type RP437 cells grown at 37°C or at 27°C. Ratio of relative mRNA levels corresponding to *cheR* and receptors at each temperature was determined using realtime PCR, and the values at 37°C were normalized by those at 27°C. **(D)** Levels of protein synthesis for plasmid-encoded Tar-YFP or CheR-YFP fusion constructs transcribed from pTrc promoter at the same induction in cultures of wild-type RP437 cells grown at 27°C (blue bars) or 37°C (pink bars). Protein expression was measured by flow cytometry and expressed in arbitrary units (AU). 'Tap' denotes fragment encoding translated *tap* gene upstream of *cheR*, whereas 'nt-tap' denotes the same fragment with mutated start codon, and 'nt-tap*' denotes the fragment that additionally carries two point mutations, −25 A->U and −34 G->C (counting from the start codon of *cheR*), which are expected to destabilize the predicted secondary structure upstream of *cheR* (Figure S3C). Constructs containing 50, 100, and 150 nucleotides, respectively, upstream of *cheR* start codon are also shown. **(E)** Temperature-dependent degradation of receptors and CheR. Cells were grown at 27°C or at 37°C to OD600 ≈ 0.48, translation was stopped, and levels of receptors (grey diamonds) and CheR (red circles) were followed over time at the respective growth temperature (27°C, open symbols; 37°C, closed symbols) using immunoblotting. **(F)** Extent of CheR (red) and receptor (grey) degradation in selected protease knockout strains. Experiments were performed for 1 hour at 37°C as in (E). CheR degradation was assayed in strains that expressed CheR and CheB ~5–6 times above the native level from pVS144 at 0.01% L-arabinose induction. See also Figure S3.